Astron. Nachr. / AN **326**, No. 3/4, 223–226 (2005) / **DOI** 10.1002/asna.200410380

Reynolds stresses – dependence on latitude

C. HUPFER[1], P. KÄPYLÄ[1,2], and M. STIX[1]

[1] Kiepenheuer-Institut für Sonnenphysik, Schöneckstr. 6, 79104 Freiburg, Germany
[2] Astronomy Division, Department of Physical Sciences, PO BOX 3000, 90014 University of Oulu, Finland

Received 5 November 2004; accepted 10 December 2004; published online 11 March 2005

Abstract. We present some results of three-dimensional hydrodynamic simulations of a compressible flow under the influence of rotation. The code implements a three-layer (stably–unstably–stably stratified) rectangular box placed at various latitudes in a convection zone of a star. We focus on the Reynolds stresses $Q_{ij} = \langle u_i' u_j' \rangle$ which in mean-field models have a crucial influence on angular momentum transport and differential rotation. Especially we examine the occurrence of a strong peak of $Q_{\theta\phi}$ at low latitude very close to the equator, which may have implications to the theory of the angular velocity profile observed on the Sun.

Key words: stars: interiors – stars: Reynolds stress – stars: differential rotation

1. Angular momentum transport

In a convection zone of a rotating star angular momentum can be transported in the radial and latitudinal directions by a variety of mechanisms. In the present contribution we consider the transport that can be described by mean-field theory (Rüdiger 1989), and restrict ourselves to the non-magnetic case. That is, we shall not calculate dynamo models. Nevertheless, the dynamo generally depends on differential rotation, and therefore on the Reynolds stress tensor which is the aim of our calculations.

In mean-field theory the transport of angular momentum is described by (e.g., Stix 2002)

$$\frac{\partial}{\partial t}(\rho s^2 \Omega) + \nabla \cdot (\rho s^2 \Omega \boldsymbol{v}_{\rm m} + \rho s \langle u_\phi' \boldsymbol{u}' \rangle) = 0\,, \tag{1}$$

where $s = r \sin\theta$ is the distance from the axis of rotation, Ω is the angular velocity, $\boldsymbol{v}_{\rm m}$ is a mean (axisymmetric) meridional circulation, and

$$Q_{ij} = \langle u_i' u_j' \rangle \tag{2}$$

is the *Reynolds stress* tensor. The prime indicates the fluctuating part of the velocity $\boldsymbol{u}$, and the angular brackets mean averaging over longitude, ϕ.

In spherical geometry, with polar coordinates (r, θ, ϕ), the non-diffusive parts of the Reynolds stress tensor are related to the Λ effect introduced by Krause & Rüdiger (1974) and Rüdiger (1980)

$$Q_{r\phi} \;=\; -\nu_{\rm r} r \sin\theta \frac{\partial \Omega}{\partial r} + \Lambda_{\rm r} \sin\theta \Omega\,, \tag{3}$$

$$Q_{\theta\phi} \;=\; -\nu_{\rm h} \sin\theta \frac{\partial \Omega}{\partial \theta} + \Lambda_{\rm h} \cos\theta \Omega\,, \tag{4}$$

where $\nu_{\rm r}$ and $\nu_{\rm h}$ are radial and horizontal eddy diffusivities, respectively.

The Reynolds stress tensor has been determined by analytical methods (Kichatinov & Rüdiger 1993) as well as in numerical studies (Pulkkinen et al. 1993, Chan 2001). The present paper belongs to the latter category.

2. The box model

Our calculations are carried out within a rectangular box that consists of three layers, as shown in Fig. 1. The middle layer, of thickness d, is convectively unstable; the lower layer, of thickness $0.68d$ is stably stratified, but the flow is allowed to overshoot into it from above. The upper layer, of thickness $0.32d$, is also stable; in addition, the upper layer is effectively cooled so that it remains nearly isothermal. We consider this upper layer mainly as a technical means to remove the heat that enters the box from below.

When applied to the Sun, the box has a vertical extent of order 100 000 km, covering the lower part of the convection zone plus a layer of convective overshooting below. The

Correspondence to: stix@kis.uni-freiburg.de

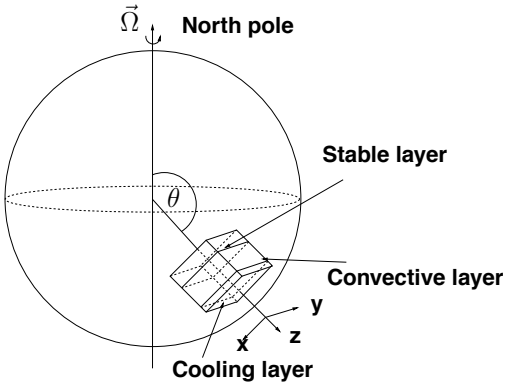

Fig. 1. The rectangular domain of computation, with three layers, here located at an intermediate latitude of the southern hemisphere.

horizontal extent is of the same order. By choosing the appropriate inclination of the rotation axis, the box can be placed at any desired latitude.

The initial setup is such that the stratification is polytropic in each of the three layers, with polytropic indices $m_1 = 3$, $m_2 = 1$, and $m_3 = \infty$, from below. The top and bottom boundaries are impermeable and stress-free, and a constant heat flux is prescribed at the bottom. At the side boundaries we impose the condition of periodicity.

2.1. Equations

We solve the conservation equations in the form

$$\frac{D\rho}{Dt} = -\boldsymbol{u}\cdot\boldsymbol{\nabla}\rho\,, \tag{5}$$

$$\rho\frac{D\boldsymbol{u}}{Dt} = -\boldsymbol{\nabla}P + \rho\boldsymbol{g} - 2\rho\boldsymbol{\Omega}\times\boldsymbol{u} + 2\nu\boldsymbol{\nabla}\cdot(\rho\underline{S})\,, \tag{6}$$

$$\rho\frac{De}{Dt} = -P\boldsymbol{\nabla}\cdot u + \boldsymbol{\nabla}\left(\kappa\boldsymbol{\nabla}e\right) + 2\nu\rho\underline{S}^2 + Q\,, \tag{7}$$

where ρ, $\boldsymbol{u}$, P, $\boldsymbol{g}$ have their usual meanings; Q is the heat sink in the upper layer. The angular velocity vector, $\boldsymbol{\Omega}$, is kept constant within the box. Kinematic viscosity and heat conductivity (representing transport by radiation) are ν and κ, respectively; we take a constant ν, while κ has different constant values in the three layers, with smooth transitions. The internal energy per unit mass is $e = c_V T$, and the rate-of-strain tensor $\underline{S}$ is given by

$$S_{ij} = \frac{1}{2}\left(u_{i,j} + u_{j,i}\right) - \frac{1}{3}\delta_{ij}u_{k,k} \qquad \underline{S}^2 = \sum_{i,j=1}^{3} S_{ij}^2\,. \tag{8}$$

The conservation equations are supplemented by the equation of state for a perfect gas,

$$P = (\gamma - 1)\,\rho e\,, \tag{9}$$

where $\gamma = c_{\rm P}/c_{\rm V} = 5/3$.

2.2. Parameters

For the actual calculations we take d as unit of length, and $t_0 = \sqrt{d/g}$ as unit of time.

The dimensionless parameters that control the calculation are the Rayleigh number

$$\mathrm{Ra} = \frac{\mathrm{d}^4\mathrm{g}\delta}{\chi\nu\mathrm{H_P}}\,, \tag{10}$$

the Prandtl number

$$\mathrm{Pr} = \frac{\nu}{\chi}\,, \tag{11}$$

and the Taylor number

$$\mathrm{Ta} = \left(\frac{2\Omega\mathrm{d}^2}{\nu}\right)^2\,. \tag{12}$$

In these expressions $\delta = 1/(m_2+1) - (\gamma-1)/\gamma = 0.1$ is the superadiabaticity of the middle (unstable) layer in the initial state, $H_{\rm P}$ is the pressure scale height in the middle of that same layer, and $\chi = \kappa/\gamma\rho_1$ is the thermal diffusivity. For our choice of parameters, we have $H_{\rm P} = 0.45d$ initially, and this remains approximately constant during the calculation. The heat conductivity κ is also from the middle layer, and $\rho_1 = \rho(z_1)$ is the density at the interface between the lower and middle layers; in the calculation ρ_1 serves as unit of density.

For the results shown below the actual values of the dimensionless control parameters are

$$\mathrm{Ra} = 250\,000\,, \qquad \mathrm{Pr} = 0.4\,, \qquad \mathrm{Ta} = 325\,000\,. \tag{13}$$

As far as the rotational influence is concerned, the inverse Rossby, or Coriolis number, $\mathrm{Co} = 2\Omega\mathrm{d}/\mathrm{u_{rms}}$, is of more interest than the Taylor number. In our model Co is a derived quantity; the chosen parameters yield $\mathrm{Co} \approx 4$, which is representative for the lower part of the solar convection zone.

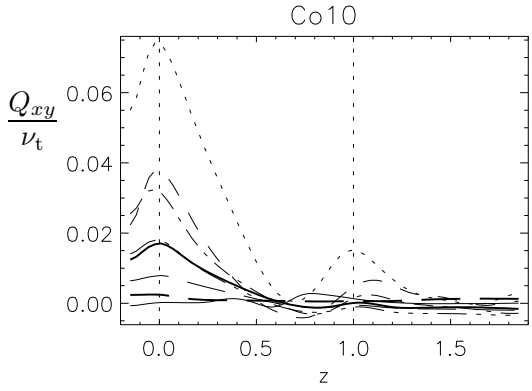

Fig. 2. The component Q_{xy} of the Reynolds stress tensor (divided by an eddy viscosity $\nu_{\rm t}$), according to Käpylä et al. (2004), as a function of depth z (here oriented inwards), for several southern latitudes. The highest maximum (*dotted*) occurs at latitude $-7.5°$. The vertical dotted lines mark the layer boundaries.

3. Results

Reynolds stresses have been derived from numerical models like the present one by a number of earlier calculations (e.g. Pulkkinen et al. 1993, Chan 2001). Chan has already inserted an extra latitude point at $11.25°$ into his model series, but it

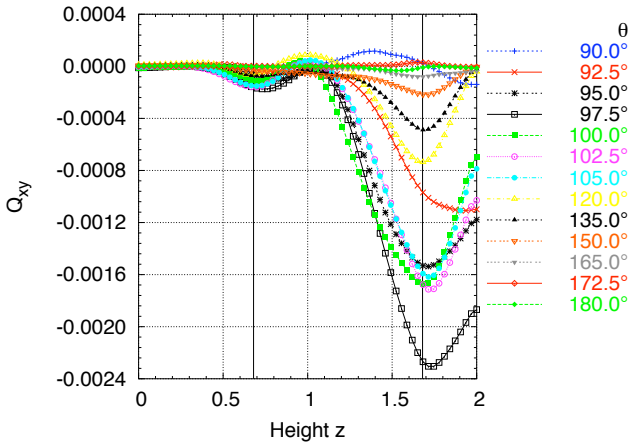

Fig. 3. (The following figures are online colour at www.an-journal.org.) The component Q_{xy} of the Reynolds stress tensor, as a function of height z, for several positions in the southern hemisphere. The sign of Q_{xy} is reversed in comparison to Fig. 2, as well as the direction of z. The vertical lines mark the layer boundaries.

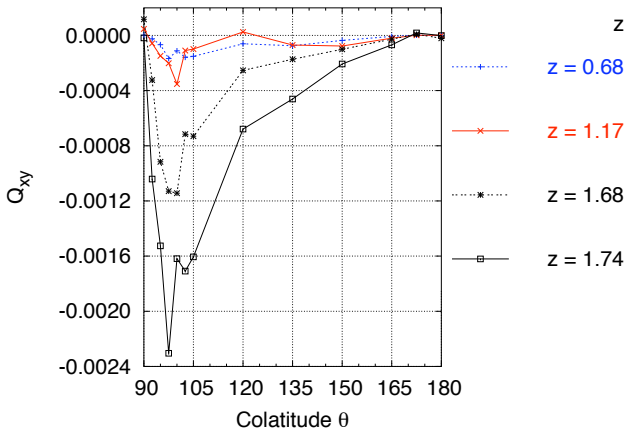

Fig. 4. Reynolds stress component Q_{xy} as a function of colatitude θ, for four different heights z in the computational box.

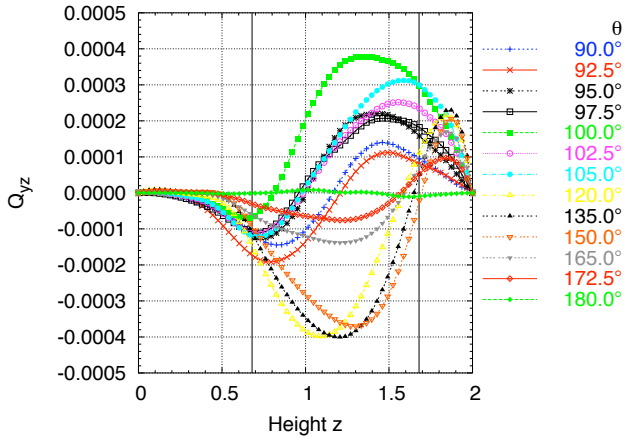

Fig. 5. The component Q_{yz} of the Reynolds stress tensor, as a function of height z, for several positions in the southern hemisphere. The coordinate z increases upwards, as in Fig. 3. Vertical lines mark the layer boundaries.

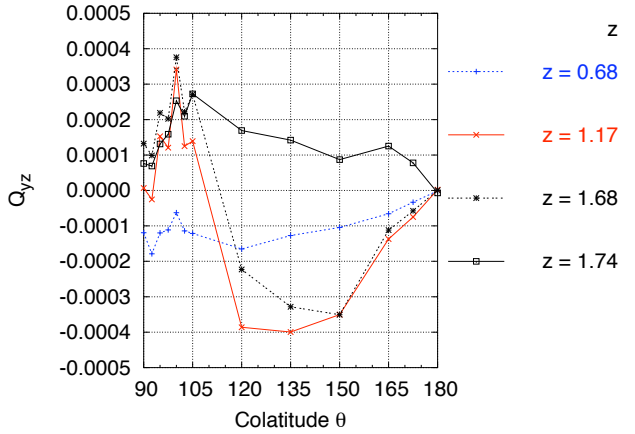

Fig. 6. Reynolds stress component Q_{yz} as a function of colatitude θ, for four different heights z in the computational box.

appears to us that the peculiar dependence on latitude that we examine in the present contribution has been noticed only recently by Käpylä et al. (2004); Figure 2 shows examples from their work, with Coriolis numbers of order 10.

Since in the model of Käpylä et al. (2004) the x-coordinate corresponds to latitude rather than colatitude θ, their positive Q_{xy} (of the southern hemisphere) corresponds to negative $Q_{\theta\phi}$. This sign is as expected. Less expected is the fact that the largest values occur so close at the equator, in particular as $Q_{\theta\phi}$ should be zero at the equator itself. In order to examine this result we did additional calculations, using a completely independent numerical code. In this code spatial derivatives are approximated by 6th-order centered differences, while the integration in time employs a 3rd-order Adams-Moulton predictor-corrector scheme (e.g., Caunt & Korpi 2001). A resolution of 64^3 grid points was used; the time step was adjusted dynamically and was of order $0.004t_0$. The calculations were parallelized with MPI and carried out on the 16-processor Linux Cluster KABUL hosted by the Kiepenheuer-Institut.

After an initial phase of $\approx$ 100 time units the model calculations reached a statistical equilibrium. The Reynolds stresses are then calculated from the velocity components as averages over the horizontal coordinates x, y,

$$\langle u_i' u_j' \rangle = \langle u_i u_j \rangle - \langle u_i \rangle \langle u_j \rangle \,. \tag{14}$$

For the results shown in Figs. 3 to 6 we have, in addition, averaged over 300 snapshots evenly distributed over a period of 1100 time units following the initial phase. The scatter of the results is of the same order as the averages shown in the figures, while the error of those averages is smaller by a factor $300^{-1/2} \approx 0.06$, apparently of the order of some of the small wiggles in Figs. 4 and 6.

Figure 3 shows the result corresponding to Fig. 2. The dependence on depth as well as the dependence on latitude is fully confirmed. In order to show the low-latitude maximum more clearly, we have added calculations for more values of θ in the close neighbourhood of the equator. Plotted at fixed height z as function of θ, the peculiar behavior of Q_{xy} is even more conspicuous (Fig. 4). The maximum at latitude 7° is most pronounced in the upper part of the box, in agreement with the result found by Käpylä et al. (2004).

The behaviour of Q_{yz}, the component related to vertical flux of angular momentum, is less clear. The absolute magnitude is less by a factor of about 5. Within the upper stable layer the sign appears to be well defined (positive); but in the bulk of the unstable layer there is a sign reversal, with negative values at intermediate and high latitude, and a positive maximum at low latitude close to the equator, (Figs. 5 and 6). Notice that, according to (3) and (4), Q_{yz} need not vanish at the equator, $\theta = \pi/2$, but Q_{xy} should do so if Ω is symmetric with respect to the equatorial plane. We have tested our code in view of the antisymmetry of Q_{xy} and the symmetry of Q_{yz} with respect to the equator.

4. Discussion

It is worth comparing our calculations with the corresponding results of Chan (2001). With weak flux (1/8) and $\Omega = 1/2$ he finds a Coriolis number around 3 (depending on latitude; notice also that his definition differs slightly from ours), which is close to our value of ≈ 4. Indeed, the latitudinal variation of the box averages of his correlations, columns (5) and (6) of Table 3, resembles that of our Q_{yz} and Q_{xy}, respectively, except for the peculiar behaviour near the equator which we found with our finer resolution. On the other hand, in spite of these similarities we should keep in mind that the two box models have some significant differences, in particular the lowest layer that allows for convective overshooting; only our model includes this layer. Incidentally, the same case of Chan (2001) has been discussed by Rüdiger et al. (2003) in connection with the mean angular velocity in the supergranular layer near the Sun's surface, although $\mathrm{Co} = 3$ appears to be too large for this application.

We have calculated the Reynolds stresses Q_{xy} and Q_{yz} in rectangular boxes under the influence of rotation, for a variety of inclination angles of the rotation axis. In dimensionless units, these two components of the Reynolds stress tensor reach maximum values of order $2 \cdot 10^{-3}$ and $4 \cdot 10^{-4}$, respectively.

For the application to the lower part of the solar convection zone we take $d = 10^8$ m and $g = 400\,\mathrm{ms}^{-2}$. Thus, our results translate to maximum values $Q_{\theta\phi} \approx 8 \cdot 10^7\,\mathrm{m}^2/\mathrm{s}^{-2}$ and $Q_{r\phi} \approx 2 \cdot 10^7\,\mathrm{m}^2/\mathrm{s}^{-2}$. This is about four orders of magnitude larger than the corresponding velocity correlations found on the surface of the Sun (e.g., Stix 2002, Table 7.3). Since those correlations are determined on intermediate and large scale, they should reflect flow properties of the deep convection zone. This discrepancy in amplitude is a consequence of the fact that the velocity amplitudes in numerical studies like the present one generally turn out too large by several orders of magnitude, due to the unrealistic choice of parameters needed for the actual computations.

If we divide the Reynolds stress tensor by the mean square velocity we obtain a dimensionless quantity; this quantity should then be compared to the corresponding ratio derived, e.g., from solar observation, and the actual values are indeed of similar magnitude.

The dependence of the Reynolds stresses on rotation and latitude should have an implication to the ensuing differential rotation. For a rate of rotation that is representative of the deep solar convection zone, with a Coriolis number of $\mathrm{Co} \approx 4$, we find a peak of Q_{xy} close to the equator. The peak is positive in the northern and negative in the southern hemisphere. We also find a peak of Q_{yz} close to the equator, positive in both hemispheres. Such a variation with latitude would mean that in an expansion of the Λ coefficients in powers of $\sin^2\theta$ one should retain more terms than the usual first two. The profile of the solar angular velocity, cf. Fig. 7, shows steep gradients, both in latitude and radius, near the equator. We wonder if these require a Reynolds stress distribution as found in our calculations. If eq. (1) is applied at the equator, $\theta = \pi/2$, and the steady state without meridional circulation is considered, we find that our numerically determined Reynolds stresses, including their spatial variation, are consistent with the angular velocity distribution shown in the figure. A more quantitative evaluation is postponed to a future contribution.

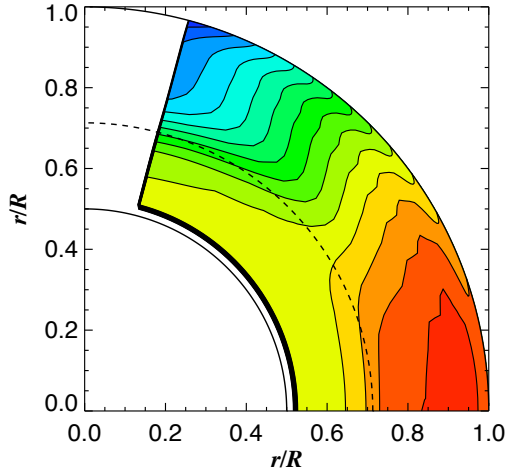

Fig. 7. Contours of constant angular velocity in the Sun, as derived by the Global Oscillation Network Group, GONG. *Dark (red)* at low latitude indicates fast rotation, *dark (blue)* at high latitude indicates slow rotation. The *dashed* curve marks the base of the convection zone. Courtesy M. Roth.

Acknowledgements. We thank Wolfgang Dobler and Mathieu Ossendrijver for investing time into discussions and help with the Linux cluster.

References

Caunt, S.E., Korpi, M.J.: 2001, A&A 369, 706
Chan, K.L.: 2001, ApJ 548, 1102
Käpylä, P.J., Korpi, M.J., Tuominen, I.: 2004, A&A 422, 793
Kichatinov, L.L., Rüdiger, G.: 1993, A&A 276, 96
Krause, F., Rüdiger, G.: 1974, AN 295, 93
Pulkkinen, P., Tuominen, I., Brandenburg, A., Nordlund, Å., Stein, R.F.: 1993, A&A 267, 265
Rüdiger, G.: 1980, GApFD 16, 239
Rüdiger, G.: 1989, *Differential Rotation and Stellar Convection*, Akademie-Verlag, Berlin
Rüdiger, G., Küker, M., Chan, K.L.: 2003, A&A 399, 743
Stix, M.: 2002, *The Sun*, 2nd ed., Springer, Berlin